http://dx.doi.org/10.21577/0103-5053.20170001

J. Braz. Chem. Soc., Vol. 28, No. 9, 1673-1681, 2017.
Printed in Brazil - ©2017 Sociedade Brasileira de Química
0103 - 5053 $6.00+0.00

Article

Microwave-Assisted Oxidation of Organic Matter Using Diluted HNO_3 under O_2 Pressure: Rationalization of the Temperature Gradient Effect for Acid Regeneration

Cezar A. Bizzi,[a] Juliano S. Barin,[b] Jussiane S. S. Oliveira,[a] Giancarlo Cravotto[c] and Erico M. M. Flores[a]*

[a]*Departamento de Química and* [b]*Departamento de Tecnologia e Ciência dos Alimentos, Universidade Federal de Santa Maria, 97105-900 Santa Maria-RS, Brazil*

[c]*Dipartimento di Scienza e Tecnologia del Farmaco, University of Turin, 10125 Turin, Italy*

Oxidation using diluted HNO_3 solution is dependent on reactions taking place in the gas phase, resulting in HNO_3 regeneration, thus allowing sub stoichiometric reactions (16.7 mmol of C oxidized with 10.4 mmol of HNO_3). Reactions for HNO_3 regeneration are dependent on temperature gradient along reaction vessel. Thermographic images were obtained of external vessel wall after 2.5, 5 and 7.5 min of heating. Temperature inside reaction vessel was directly measured using a sapphire thermocouple in four different depth (3, 6, 12 and 16 cm). Reactions under inert atmosphere (7.5 bar Ar) were evaluated and normally presented higher temperature gradient than that performed with O_2 pressure, since HNO_3 regeneration reactions are exothermic. A better understanding of the regeneration of HNO_3 and the dependence on the whole reaction vessel temperature in this system was possible combined to residual carbon content and residual acidity measurements to estimate the extent of organic matter oxidation.

Keywords: microwave-assisted oxidation, diluted HNO_3, IR thermal imaging, temperature gradient, gas phase reaction

Introduction

Organic matter oxidation has been considered crucial to ensure reliable results especially since the advent of inductively coupled plasma (ICP)-based techniques for the analysis of organic samples, which normally use nebulizers for the introduction of liquid or dissolved/digested samples. High digestion efficiency of organic matrices is still a requirement for minimizing interferences caused by matrix effect, in elemental determination.[1,2] In recent years, a great effort has been done for achieving better digestion efficiency and avoiding the use of concentrated reagents. Several improvements were obtained when using diluted acids associated with powerful equipment,[3] as well as by powering the digestion reaction with oxygen, as an auxiliary reagent.[4,5]

The oxidation of organic matter using diluted solutions of HNO_3 (equation 1)[6,7] is related to a series of side reactions that simultaneously happen and lead to HNO_3 regeneration (equations 2 to 4).[8-11] The first requirement for these reactions is a sufficient amount of O_2 that must be present in the gas phase (equation 2). After the oxidation of $NO_{(g)}$ to $NO_{2(g)}$, the latter is absorbed by solution and a disproportionation reaction occurs producing HNO_3 and HNO_2 (equation 3). The HNO_3 produced may restart the oxidation cycle of organic matter (equation 1). Since the reaction is performed in closed vessels, this sequence of reactions will occur as long as O_2 is present in the reaction vessel, as shown in previous investigations.[12]

$$(CH_2)_n + 2HNO_{3(aq)} \rightarrow CO_{2(g)} + 2NO_{(g)} + 2H_2O_{(l)} \quad (1)$$
$$2NO_{(g)} + O_{2(g)} \rightarrow 2NO_{2(g)} \quad (2)$$
$$2NO_{2(g)} + H_2O_{(l)} \rightarrow HNO_{3(aq)} + HNO_{2(aq)} \quad (3)$$
$$2HNO_{2(aq)} \rightarrow H_2O_{(l)} + NO_{2(g)} + NO_{(g)} \quad (4)$$

It has also been shown that the occurrence of equation 3 is dependent on the second requirement: the existence of a temperature gradient along the reaction vessel.[9,13] The temperature gradient is related to the difference in liquid and gas phase temperatures in a

*e-mail: cezar.bizzi@gmail.com

reaction heated by microwaves (MW).[14] A number of studies have investigated the factors that promote HNO_3 regeneration. The use of diluted HNO_3 as an oxidant of organic matrix under both MW and conventional heating has been studied.[9] Although the temperature gradient was not determined, the higher efficiency of organic matter oxidation obtained under MW was attributed to the presence of a cool gas phase that caused the condensation of NO oxidation products.

The existence of a temperature gradient has also been correlated to a reduction in internal pressure for reactions performed in a closed MW heating system. It was assumed that the cooler vessel walls contributed to reduce the solvent partial pressure due to the increased condensation rate.[15] This allows MW to irradiate longer, thus improving the efficiency of organic matter oxidation. A reduction in the solvent partial pressure has been studied and intensified by carrying out the simultaneous cooling of the reaction vessel in the MW-assisted oxidation of organic matter.[16] As reported, a higher air stream outside the reaction vessel and higher temperature in the solution lead to higher organic matter oxidation efficiency. Both works[15,16] found that higher oxidation reaction efficiency was related to a simultaneous cooling promoted by temperature gradient along the digestion vessel.

An evaluation of the real effect of a temperature gradient along the reaction vessel has been carried out using thermographic imaging (infrared images).[17] Information was obtained from the external part of the reaction vessel, while the system was simultaneously subjected to a cooling air stream. Although this protocol may be prone to interferences,[18] the information obtained was enough to correlate the improvement in oxidation efficiency to a reduction in gas phase temperature.[17]

It is therefore possible to hypothesize that HNO_3 regeneration is related to the temperature gradient. This has been generally accepted, despite the fact that temperature has never been directly recorded in the gas phase of an O_2-pressurized reaction vessel. The present work thus aims to combine information on the external temperature gradient with internal values. The former was recorded using an infrared camera which provided an overall view of the temperature gradient. The internal gradient was measured using a thermocouple and allowed to obtain the temperature directly where the HNO_3 regeneration reactions takes place. The temperature gradient, as well as its dependence on reaction time and gas phase composition, was matched with residual carbon content (RCC) and residual acidity values in order to better understand the HNO_3 regeneration reactions using diluted HNO_3 solutions for organic matter oxidation. Therefore, this information can help the planning and development of microwave-assisted reactions in many fields of chemistry, especially those related to analytical chemistry.

Experimental

Instrumentation

All sample digestion experiments (organic matter oxidation) were performed using a MW oven (Multiwave 3000 Microwave Sample Preparation System, Anton Paar, Graz, Austria) equipped with eight high-pressure quartz vessels (80 mL). Maximum operational temperature and pressure were set at 280 ºC and 80 bar, respectively. Pressure and temperature were monitored in each vessel at every run.

The temperature along the external vessel surface was measured using an infrared camera (IR, SC-305, Flir, Sweden) with a spectral range of between 7.5 and 13 μm and at 0.05 ºC thermal sensitivity. The software FLIR ResearchIR was used for image analysis. The evaluation of internal reaction vessel temperature (liquid and gas phase) was performed using a thermocouple (thermocouple type K, TM 201/16.394-500, Salcas, Brazil) with an operational range of −200 up to 800 ºC, which was positioned inside the vessel using a sapphire immersion tube with a special seal (immersion tube with seal XQ, Cat. No. 13,924, Anton Paar).

Residual carbon content (RCC, %)[19] in final digests was calculated by means of C determination using an inductively coupled plasma optical emission spectrometer (ICP OES, PerkinElmer, Optima 4200 DV, Waltham, USA)[20] which was related to the initial amount of C in the organic matrix. In order to remove the volatile carbon compounds before RCC determination, sample aliquots were purged for 2 min with 0.1 mL min^{-1} of argon (99.998%, White Martins-Praxair, São Paulo, Brazil). Argon was also used for plasma generation in ICP OES determination, nebulization and for reactions performed under an inert atmosphere. Oxygen (99.6%, White Martins-Praxair) was used for oxidant atmosphere reactions.

The conditions for all procedures performed under oxygen or argon pressure were based on previous studies.[12,21] These operations were selected according to the recommendations of the MW oven manufacturer[22] and safety of operator.

Results for residual acidity were obtained using a titration system (Titrando 836, Metrohm, Herisau, Switzerland), which was equipped with a magnetic stirrer (module 803 Ti Stand), 20 mL burette (Dosino 800) and pH electrode (LL Electrode plus, model 6.0262.100).

Samples, reagents and standards

All experiments performed for temperature gradient evaluation were carried out using whole milk powder (51% of C), which was purchased from a local market. Samples were dried to constant mass at 105 ºC, using a conventional oven, prior to the oxidation reaction (model 400/2ND, Nova Ética, Vargem Grande Paulista, SP, Brazil). Samples were weighed using an analytical balance (AY 220, max. 220 g, 0.1 mg of resolution, Shimadzu, Kyoto, Japan).

Distilled-deionized water (Milli-Q, 18.2 MΩ cm, Millipore, Billerica, MA, USA) and analytical-grade nitric acid (Merck, Darmstadt, Germany) were used to prepare samples and standards. Carbon reference solutions used for external calibration for C determination were prepared via the dissolution of citric acid (Merck) in water (from 10 up to 500 mg L^{-1} of C). Yttrium (1.0 mg L^{-1}, Spex CertPrep, Metuchen, NJ, USA) was used as the internal standard for C determination. Glass and quartz materials were soaked in 1.4 mol L^{-1} HNO_3 for 24 h and washed with water before use.

MW-assisted oxidation

Samples (up to 500 mg, 21.2 mmol of C) were transferred to quartz vessels and digested using 2 mol L^{-1} HNO_3 (6 mL, 12 mmol). When the oxidation reaction was carried out using an oxidant atmosphere, vessels were pressurized with 7.5 bar of oxygen. For comparison purposes, sample oxidation was performed with inert gas pressure (Ar, 7.5 bar). After placing the vessels inside the oven, the MW irradiation program was started by applying (*i*) 1000 W with a ramp of 5 min; (*ii*) 1000 W for 10 min and (*iii*) 0 W for 20 min.[21]

After oxidation, the pressure of each vessel was carefully released. Each run was performed using four vessels in this work. Final digests were evaluated using ICP OES for C determination. Residual acidity was evaluated by titration. Statistical evaluation was performed using the Student's *t*-test, (GraphPad InStat Software Inc, Version 3.00, 1997) with a significance level of $p > 0.05$ for all comparisons.

Infrared thermal imaging measurements

Infrared images were obtained at different reaction times (2.5, 5.0 and 7.5 min), but did not cover the entire heating program for safety reasons. Vessels were covered with a homemade and specially designed protective casing with a window of 13.5 cm height and 4.0 cm width to allow the images to be recorded during irradiation (Figure S1, Supplementary Information section). This modification in the protective casing was necessary in order to allow the acquisition of IR information from the vessel external wall surface. Despite the open window represents almost one third of the total vessel surface, it was not considered a representative source of error due to the very poor thermal conductivity of air. In this sense, it might be assumed that any leakage of thermal radiation was just enough for obtaining the IR information, but not enough for representative changes in the temperature of the vessel wall.

The IR camera was positioned in front of the frontal door of MW oven at a distance of 60 cm of reaction vessel. The relative humidity and ambient atmosphere were controlled and informed to the IR camera software for automatic settings. Quartz vessel emissivity was determined against a blackbody, as recommended by IR camera manufacturer. These information were taken into account during image processing. Thermographic images were obtained after the heating program has been stopped and the oven door was opened to allow measurement at pre-determined times (2.5, 5.0 and 7.5 min). Considering all involved steps, the delay in obtaining the images was always lower than 5 s. The IR camera operator was positioned behind polycarbonate protection in order to assure safety during measurements.

Thermocouple measurements of temperature in the liquid and gas phases

Despite the temperature profile being recorded in the external part of the vessel, an evaluation of the temperature inside reaction vessel was also performed. A thermocouple sensor was thus positioned inside the vessel using a sapphire immersion tube that had been specially modified to obtain temperatures at varying reaction vessel depths, as presented in Figure 1. For each height where temperature was measured, the sapphire immersion tube was made in the proper size (Figure S2, Supplementary Information section). In addition, it is possible to suppose that complete sapphire tube was in thermal equilibrium with vessel internal environment, once it is a part of the system since the beginning of the reaction. Sapphire immersion tube has a very poor thermal conductivity being an important contribution for avoiding any leakage of heat during MW irradiation and temperature measurement. In addition, the used system is commercially available, and the only modification was related to its size, which makes possible to assume that accurate information for internal temperature was obtained.

In this sense, four depths were evaluated (3, 6, 12 and 16 cm), followed by four sapphire immersion tube lengths (Figure S2, Supplementary Information section). Each depth-relative temperature was obtained after 2.5, 5 and 7.5 min of reaction, as in the IR thermal imaging

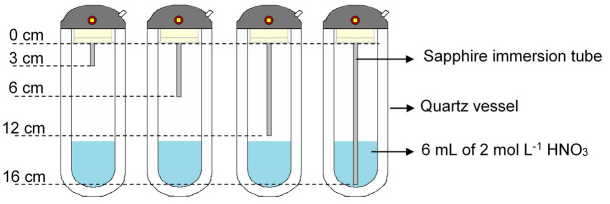

Figure 1. Reaction vessel with immersion tube used for temperature measurement using a thermocouple sensor. Temperature was obtained from the liquid phase (16 cm depth) and from the gas phase (3, 6 and 12 cm depth) every 2.5, 5 and 7.5 min of MW irradiation.

measurements. In order to avoid MW electromagnetic field interference in the thermocouple response, temperature information was obtained after MW heating has been stopped, and the thermocouple was subsequently positioned inside the immersion tube. The whole procedure (stopping MW heating and thermocouple positioning into immersion tube) lasted no more than 10 s. This delay was considered to have no effect on the temperature measurement once it stayed constant for the subsequent 30 s or longer.

Another important aspect is that for such evaluation a commercial available protective casing was used. Since the quartz material present a relative poor thermal conductivity, as well as a wall thickness of 8 mm, it was assumed that the external environment did not affect the internal one, where information was acquired using a thermocouple. It allowed to use this information in combination with that obtained by IR camera (external surface information) for better understanding the effect of temperature gradient.

Results and Discussion

In a general procedure for the oxidation of organic matrices, the higher the temperature, the better is the oxidation efficiency. However, the use of oxygen as an auxiliary reagent makes possible the organic matter oxidation using diluted HNO_3 without impairing digestion efficiency. In this sense, a clear understanding of the chemical reactions that occur in digestion vessel, mainly those happening in the gas phase, becomes crucial. Although these reactions are time dependent, they are also related to the temperature gradient inside the digestion vessel.[16] In order to better elucidate this factor, temperature gradients were evaluated under several gas phase compositions (Ar and O_2 pressure).

Evaluation of the effect of the irradiation program on the oxidation of organic matter and its dependency on gas phase composition

The progress of sample oxidation using diluted HNO_3, pressurized with O_2, and its dependence on reaction time and temperature gradient were evaluated. The final appearance of the resultant reaction solution was therefore monitored after 2.5, 5, 7.5 and 15 min of MW assisted digestion using diluted HNO_3 (2 mol L^{-1}).

As presented in Figure 2, the oxidation of organic matter under oxygen atmosphere was almost complete as digestion time was increased. When the irradiation time of the O_2 pressure (7.5 bar) reaction was increased from 2.5 to 5 min, the amount of suspended particles decreased and the final solution was partly translucent. At 7.5 min, although the final solution was yellowish in appearance, there were no longer any solid suspended particles. From 7.5 up to 15 min heating, the final solution became completely clear (RCC was about 21%).

The same behavior was not observed when digestion was performed under inert atmosphere (Ar, 7.5 bar). As also observed in Figure 2, digestion was not complete and the final solution presented a brown color, even at the end of the oxidation reaction (15 min of MW heating), showing that the organic compounds were just partially oxidized (RCC > 80%).

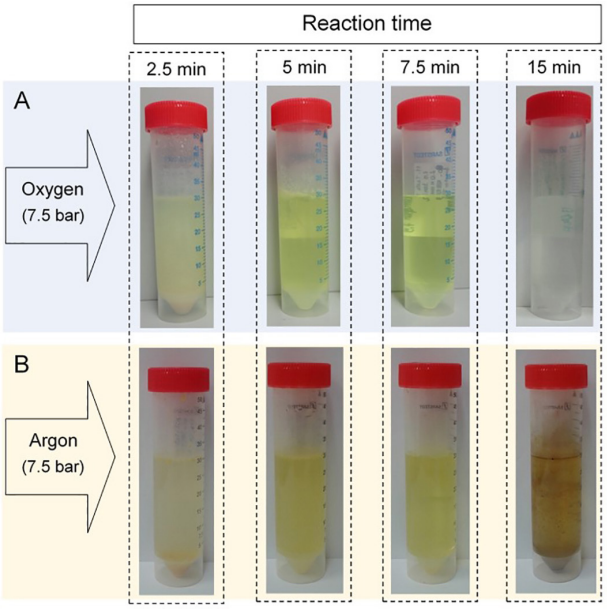

Figure 2. Appearance of final solutions obtained after 2.5, 5, 7.5 and 15 min of MW. (A) Oxidation performed under oxygen pressure (7.5 bar); (B) oxidation performed under inert gas phase composition (Ar, 7.5 bar). Both procedures were performed using 500 mg whole milk powder and 6 mL of 2 mol L^{-1} HNO_3.

In the present work, it was clear that the oxidation of organic matter was more dependent on gas phase composition than MW heating time. This means that, depending on the composition of the gas phase, an increase in reaction time has no effect on the final result. On the other hand, when enough O_2 is present in the gas

phase, which causes the HNO_3 regeneration reaction, it is possible to achieve a complete oxidation of the organic compounds present in sample in a time dependent way. Such differences in oxidation behavior can be caused by a number of factors, mainly those responsible for allowing the reactions between NO and O_2 in the gas phase (equation 2), such as temperature gradient and oxygen concentration. In order to better elucidate the role of these parameters, they are further correlated and discussed.

Evaluation of temperature gradient with varying gas phase composition

The temperature gradient was investigated, as well as its influence on the completion of the oxidation of organic matter, using two different approaches: (*i*) thermal images (thermography) using an infrared camera that provided information about the external vessel surface and (*ii*) thermocouple, which allowed to obtain information directly inside of the reaction vessel (liquid and gas phase). These evaluations were performed under both O_2 and Ar pressure (7.5 bar in each case), as discussed in the sequence of this work.

Evaluation of gradient temperature by infrared thermal imaging

The extent of organic matter oxidation efficiency that occurs when HNO_3 is used depends on a series of reactions that take place in the reaction vessel that, in turn, depend on the presence of oxygen.[17] These reactions are also dependent on the temperature gradient along the reaction vessel.[12,16] The temperature gradient (from the liquid phase, at the bottom, to the gas phase, at the top) was therefore evaluated while the gas phase composition was changed from inert to oxidant (7.5 bar of Ar and O_2, respectively).

Firstly, an IR camera was used to evaluate the temperature gradient of the external reaction vessel surface; thermographic images are present in Figure 3. The images were obtained after 2.5, 5 and 7.5 min of reaction (same times presented in Figure 2). As can be seen, the bottom of the digestion vessel (in contact with the liquid phase, temperature represented by T_{bottom}) was always at a higher temperature than the top (temperature represented by T_{up}) when it was pressurized with an inert gas (Ar, 7.5 bar). Additionally, a decrease in the gradient temperature ($\Delta T = T_{bottom} - T_{up}$) was observed from 2.5 to 7.5 min (ΔT of 40.0 and 9.9 ºC, respectively). This result was expected as the reaction vessel is MW transparent and only the solution present at the bottom contributes to increase the temperature in the system. After some time under MW irradiation, the whole vessel starts to be conductively heated, decreasing the temperature gradient.

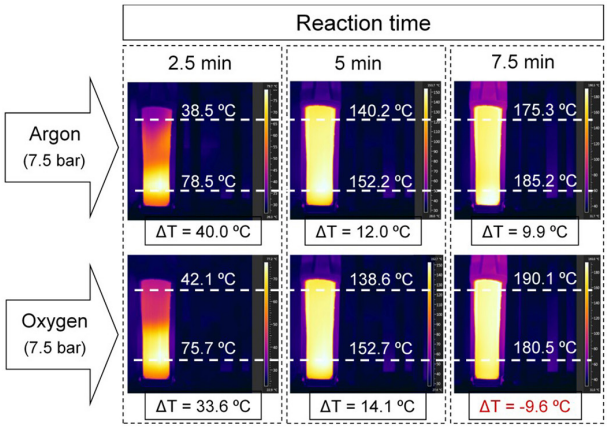

Figure 3. External surface profile of vessel temperature obtained during reactions pressurized with 7.5 bar of Ar and O_2. White dashed lines indicate the average region where the temperature was recorded. Above each image is shown the difference between the temperatures at the top and bottom of the reaction vessel ($\Delta T = T_{bottom} - T_{up}$). The temperature gradient was evaluated using 6 mL of 2 mol L^{-1} HNO_3 for the digestion of 500 mg whole milk powder, after 2.5, 5 and 7.5 min of MW heating.

While the behavior observed when the oxidation reaction was performed under inert atmosphere (7.5 bar of Ar) was predictable, the same behavior was not observed for the reaction carried out under 7.5 bar of O_2 (Figure 3). The bottom of the vessel presented higher temperature than the upper part just after 2.5 and 5 min of MW heating (ΔT of 33.6 and 14.1 ºC, respectively). After 7.5 min, the top of the vessel (in contact with gas phase) presented higher temperature than the bottom ($\Delta T = -9.6$ ºC), as also presented in Figure 4.

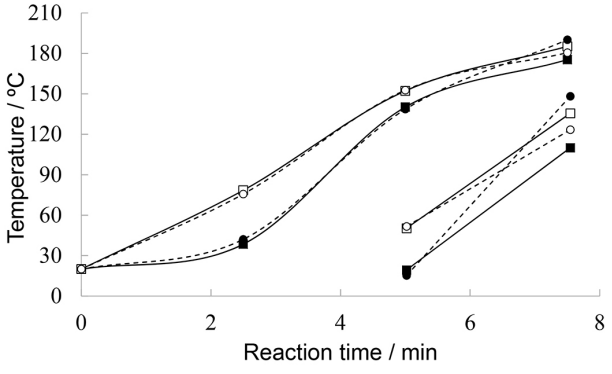

Figure 4. Reaction vessel external temperature according to heating time (2.5, 5 and 7.5 min). Temperature was recorded using an infrared camera for reactions performed with: 7.5 bar of Ar (continuous line) (■) in the area related to the gas phase and (□) in the area related to the liquid phase; 7.5 bar of O_2 (dashed line) (●) in the area related to the gas phase and (○) in the area related to the liquid phase. In detail, it is possible to see that the temperature in the gas phase becomes higher than that in liquid phase for reaction performed under O_2 pressure. Oxidation reaction using 6 mL of 2 mol L^{-1} HNO_3 for the digestion of 500 mg whole milk powder (n = 3).

Reaction performed under O_2 pressure improved oxidation of organic matter due to HNO_3 *in situ* regeneration. In this condition, it is observed a further increase in condensation rate on the vessel wall. Despite release heat, condensation also contributes for increase the amount of H_2O and HNO_3 adsorbed onto vessel wall, which starts to act as MW absorber and explain the higher temperature after 7.5 min of MW heating.

In a MW heated reaction performed at high pressure and high temperature, pressure control is a practical way for predicting what is happening inside reaction vessel. The increase in pressure is related to solvent evaporation (H_2O and HNO_3 partial pressures), as well as to reaction products (mainly CO_2 and NO partial pressures).[15,16] Despite it is considered an important aspect, once the saturation of the gas phase with vapor can result in MW heating, both vessels (under Ar and O_2 pressure) presented similar pressure after 7.5 min of MW heating (45.5 and 46.9 bar, respectively). Also worth noting is the fact that, as presented in Figure 2, the reactions were at different stages of organic matter oxidation after 7.5 min of heating. This information suggests that the gas phase composition of the O_2 pressure reaction is different, even under similar pressures of O_2 and Ar. The temperature was therefore measured internally in order to provide more accurate information, as well as to shed light on the possible relationship between the temperature gradient and the nitric acid regeneration reactions.

The use of a thermocouple for evaluating internal temperature

The temperature inside the reaction vessel was obtained at four different depths (Figure 1). Three of them were in contact with the gas phase (3, 6 and 12 cm) and one was in the liquid phase (16 cm). As in previous evaluations, the temperature information of each level was obtained after 2.5, 5 and 7.5 min of reaction (Table 1), as we aimed to correlate this information with that obtained using the IR camera.

The temperature recorded in the liquid phase was always higher than in the gas phase. The temperature gradually decreased while increasing thermocouple distance from the liquid phase (thermocouple positioned from 12 up to 3 cm from the top). This predictable behavior was similar for both oxidant and inert gas phase compositions, across all MW irradiation times. Despite the similarities mentioned above, a slight difference in temperature profile was observed between the two gas phase compositions. Figure 5 shows this difference of temperature, recorded by thermocouples positioned at 16 cm (bottom, liquid phase) and 3 cm (top, gas phase), as a temperature gradient along the reaction vessel.

After 5 and 7.5 min of heating, a distinct trend in the temperature profile (at the same depth) was observed for reactions pressurized with Ar and O_2 (Figure 5). When the gas phase was pressurized with O_2, the temperature was relatively higher than that in the system pressurized with Ar. The information recorded at 5 min of reaction presents a slightly difference when looking to the liquid phase. Reaction under O_2 pressure presented lower temperature than that observed for Ar (119 ± 3 and 139 ± 5 ºC, respectively). Both reactions were at very different stages when considering the extension of organic matter oxidation (as can be understood from Figure 2). When Ar was used, the oxidation of organic matter slowly moves to

Table 1. Evaluation of the temperature inside the reaction vessel with inert or oxidant gas phase compositions (Ar or O_2, pressure of 7.5 bar), obtained using a thermocouple. Four depths were evaluated (3, 6, 12 and 16 cm) after 2.5, 5 and 7.5 min of MW heating. The temperature gradient was expressed as the difference between data obtained at 16 and 3 cm ($\Delta T = T_{16cm} - T_{3cm}$; where $T_{16cm} = T_{bottom}$ and $T_{3cm} = T_{up}$). The oxidation reaction was performed using 6 mL of 2 mol L^{-1} HNO_3 for digestion of 500 mg whole milk powder (n = 3)

Gas phase composition	Thermocouple depth / cm	Temperature / ºC		
		Heating time (2.5 min)	Heating time (5 min)	Heating time (7.5 min)
Ar (7.5 bar)	3	28 ± 1	83 ± 2	156 ± 4
	6	37 ± 1	95 ± 2	165 ± 4
	12	47 ± 2	110 ± 3	177 ± 4
	16	55 ± 2	139 ± 5	202 ± 5
ΔT (Ar pressure) = $T_{16cm} - T_{3cm}$		27	56	46
O_2 (7.5 bar)	3	33 ± 2	91 ± 5	174 ± 3
	6	38 ± 1	101 ± 2	180 ± 3
	12	51 ± 2	106 ± 3	186 ± 4
	16	50 ± 2	119 ± 3	202 ± 3
ΔT (O_2 pressure) = $T_{16cm} - T_{3cm}$		17	28	28

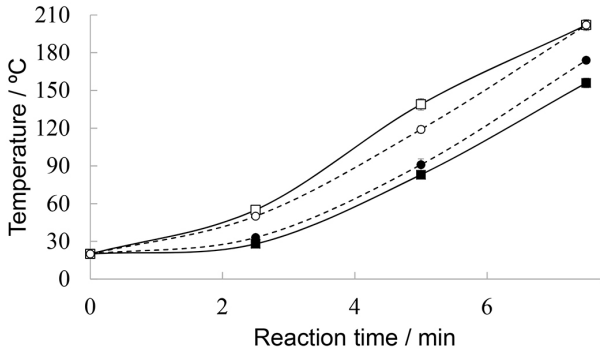

Figure 5. Internal reaction vessel temperature according to heating time (2.5, 5 and 7.5 min). Temperature was recorded using a thermocouple for reactions performed with: 7.5 bar of Ar (continuous line) at (■) 3 cm depth, gas phase and (□) 16 cm depth, liquid phase; 7.5 bar of O_2 (dashed line) at (●) 3 cm depth, gas phase and (○) 16 cm depth, liquid phase. Oxidation reaction using 6 mL 2 mol L^{-1} HNO_3 for the digestion of 500 mg whole milk powder (n = 3).

the equilibrium, since the HNO_3 is consumed and is not recycled anymore. This aspect leads to less CO_2 production and, consequently, a reduction in the rate of pressure increase. It allows MW irradiate longer in the beginning of oxidation (up to approximately 5 min, as experimentally observed), which might explain the higher temperature when reaction was performed under inert gas phase.

Although the temperatures in liquid phase (Ar and O_2 reactions) were the same after 7.5 min of irradiation, the temperature in the gas phase was higher for vessels pressurized with O_2 when compared with those pressurized with Ar. There were a higher temperature gradient for reactions under an inert atmosphere (ΔT = 46 and 28 ºC, for Ar and O_2, respectively).

The most interesting aspect to be pointed out about the gas phase can be found in the O_2 pressure reactions. They normally present higher temperature than under inert atmosphere. Such higher temperatures observed in the oxidant gas phase can be explained by the HNO_3 regeneration reactions. These reactions, that take place in the gas phase, are exothermic (equations 5 and 6),[23-25] and occur only in the presence of O_2.

$$2NO_{(g)} + O_{2(g)} \rightarrow 2NO_{2(g)} \qquad \Delta_r H^o = -113.3 \text{ kJ mol}^{-1} \quad (5)$$

$$3NO_{2(g)} + H_2O_{(g)} \rightarrow 2HNO_{3(l)} + NO_{(g)}$$
$$\Delta_r H^o = -134.6 \text{ kJ mol}^{-1} \quad (6)$$

Besides contributing to the increase in gas phase temperature, they are also responsible for intensifying the oxidation of organic matter present in the reaction vessel. This hypothesis can be confirmed by the RCC values for the reactions performed under O_2 and Ar pressure (RCC of 21 and > 80%, respectively). Residual acidity also provided important information about nitric acid regeneration. Whereas organic material is oxidized to CO_2, HNO_3 is consumed during reaction and its products are released into the atmosphere as $NO_{(g)}$ (equation 1). Considering the initial amount of HNO_3 (12 mmol each reaction), only 13.2% (1.58 mmol HNO_3, reaction under O_2 atmosphere) and 10.7% (1.28 mmol HNO_3, reaction under Ar atmosphere) remained in the final solution after organic matter oxidation. Despite the closer residual acidity values, only the O_2 pressure reaction was efficient in oxidizing organic matter (low RCC value), featuring the reuse cycle of HNO_3.

By considering both values (RCC and residual acidity), it is evident that the oxidation of organic matter was more efficient when the oxidation reaction was performed under O_2 pressure and the residual acidity was also slightly higher. Taking into account the initial amount of C (21.2 mmol) and HNO_3 (12 mmol), the oxidation reactions under oxygenated atmosphere occurred in sub stoichiometric amounts. Based on residual amount of C (21%, 4.45 mmol) and HNO_3 (13.2%, 1.58 mmol), approximately 16.7 mmol of C were oxidized with 10.4 mmol of HNO_3. It is a clear indication that the improvement in the organic matter oxidation was a result of HNO_3 regeneration, which probably has NO as catalyst and O_2 as consumable oxidizing agent.[26] This also reinforces the hypothesis that the higher temperature in the gas phase for the O_2 reaction is a consequence of those exothermic reactions.

Correlation of temperature gradient obtained by thermographic images and thermocouple measurements

Results from both approaches show that there is a temperature gradient along the closed vessel during MW heated oxidation reactions. However, as previously reported,[18] they do not provide exactly the same information once the thermographic images were obtained for the external surface of the reaction vessel. Information must, therefore, be combined for proper interpretation about what happens when oxidation reactions take place in the O_2 pressurized system.

The adverse results obtained by means of thermography, after 7.5 min of oxidation MW heated reaction under O_2 pressure (gas phase hotter than liquid phase), can be explained by looking at the heat released by the HNO_3 regeneration reaction. The temperature recorded using a thermocouple (directly in the gas phase) when reactions took place under O_2 pressure was normally higher than that under Ar pressure. It suggests that these reactions occur in the gas phase and heat is released into the system. It is confirmed when evaluating the thermodynamic aspects related to the reactions taking place in the gas phase, which are related to NO oxidation (equation 5) and further reaction

with water to generate HNO_3 (equation 6). Both reactions are exothermic, and the existence of an intense temperature gradient (with cooler gas phase) might drive the extension of each reaction. This result corroborates those obtained when reactions of organic matter oxidation with diluted HNO_3 assisted by MW heating were simultaneously cooled.[16] It is possible to suppose that the higher the heat exchange (by applying an external cooling), the better the digestion efficiency, being dependent on the improvement in the HNO_3 regeneration reaction.

All products that came from HNO_3 regeneration reactions (equation 2: NO_2; equation 3: HNO_3 and HNO_2; and equation 4: H_2O, NO_2 and NO) are prone to condensation on the cooler vessel wall (these products are mainly formed when reaction occurs in the presence of O_2). Despite condensation lead to a reduction in the total pressure of closed systems, it also contributes for heat releasing. Consequently, the vessel wall starts to be heated not only by conduction, but also by the heat released by the product condensation phenomenon. The higher the amount of products condensed on the vessel wall, the more MW will start to be absorbed, resulting in an additional temperature increase. In addition, the extension of organic matter oxidation determines the rate of CO_2 production that contributes for pressure increasing. This must be considered while looking for gaseous products condensation phenomena. Both aspects, products prone to condensation and higher production of CO_2, are mainly observed in the reactions performed under O_2 rich atmosphere.

The existence of a temperature gradient along reactional vessel is an important feature when exothermic reactions take place in the gas phase, as those observed for HNO_3 regeneration. Since the comprehension of these reactions lead to milder reactional conditions, controlling the heat exchange by intensifying the temperature gradient starts to be an interesting approach.

Conclusions

In this work, two temperature measurement systems were used to understand the influence of temperature gradient along the reaction vessel on HNO_3 regeneration and oxidation efficiency. Thermographic images of the external walls of the reaction vessel clearly showed the temperature distribution along the digestion vessel. A specially designed thermocouple directly measured the temperature inside the reaction vessel, which was positioned in contact with the liquid phase (one depth) and gas phase (three different depths). Each temperature value was acquired immediately after the MW irradiation has been stopped. It is thought that this approach would provide information quite closer to the real temperature inside the digestion system, without MW and field interferences. This information then contributed for interpreting how the reactions of HNO_3 regeneration happen in an oxygenated atmosphere. The differences between information obtained using an infrared camera and a thermocouple helped to better explain the reactions occurring during the oxidation of organic material. Both types of information corroborate the mechanism that has already been presented for HNO_3 regeneration reaction in O_2 rich atmospheres. This understanding certainly will contribute for developing specially designed MW reactors, saving energy and improving reactions efficiency. The possibility of intensifying the HNO_3 *in situ* recycling leads to further reductions in the amounts of reagents required for organic matter oxidation, contributing for less residues generation and driven chemical protocols towards to green chemistry requirements.

Supplementary Information

Supplementary information with pictures of reaction vessel with protective casing especially designed for infrared images recording, as well as pictures of sapphire immersion tube to insert a thermocouple sensor for temperature measurement in different depth are available free of charge at http://jbcs.sbq.org.br as PDF file.

Acknowledgments

The authors are grateful to FAPERGS, INCT-Bioanalítica, CNPq and CAPES for supporting this study and the scientists exchange project World Wide Style (WWS2-University of Turin).

References

1. Daniel, M. M.; Batchelor, J. D.; Rhoades, C. B.; Jones, B. T.; *At. Spectrosc.* **1998**, *19*, 198.
2. Knapp, G.; Maichin, B.; Baumgartner, U.; *At. Spectrosc.* **1998**, *19*, 220.
3. Nóbrega, J. A.; Pirola, C.; Fialho, L. L.; Rota, G.; de Campos Jordão, C. E. K. M. A.; Pollo, F.; *Talanta* **2012**, *98*, 272.
4. Crizel, M. G.; Hartwig, C. A.; Novo, D. L. R.; Toralles, I. G.; Schmidt, L.; Muller, E. I.; Mesko, M. F.; *Anal. Methods* **2015**, *7*, 4315.
5. Hartwig, C. A.; Pereira, R. M.; Rondan, F. S.; Cruz, S. M.; Duarte, F. A.; Flores, E. M. M.; Mesko, M. F.; *J. Anal. At. Spectrom.* **2016**, *31*, 523.
6. Gonzalez, M. H.; Souza, G. B.; Oliveira, R. V.; Forato, L. A.; Nóbrega, J. A.; Nogueira, A. R. A.; *Talanta* **2009**, *79*, 396.

7. Araújo, G. C. L.; Gonzalez, M. H.; Ferreira, A. G.; Nogueira, A. R. A.; Nóbrega, J. A.; *Spectrochim. Acta, Part B* **2002**, *57*, 2121.
8. Kingston, H. M.; Jassie, L. B.; *Anal. Chem.* **1986**, *58*, 2534.
9. Castro, J. T.; Santos, E. C.; Santos, W. P. C.; Costa, L. M.; Korn, M.; Nóbrega, J. A.; Korn, M. G. A.; *Talanta* **2009**, *78*, 1378.
10. Trevizan, L. C.; Donati, G. L.; Nogueira, A. R. A.; Nóbrega, J. A. In *Trends in Sample Preparation*; Arruda, M. A. Z., ed.; Nova Science Publishers: New York, 2007, p. 29.
11. Lee, J. D.; *Concise Inorganic Chemistry*, 5th ed.; Wiley India Pvt. Limited: New Delhi, 2008, p. 1028.
12. Bizzi, C. A.; Flores, E. M. M.; Barin, J. S.; Garcia, E. E.; Nóbrega, J. A.; *Microchem. J.* **2011**, *99*, 193.
13. Knapp, G.; Panholzer, F.; Schalk, A.; Kettisch, P. In *Microwave Enhanced Chemistry: Fundamentals, Sample Preparation, and Applications*; Kingston, H. M.; Haswell, S. J., eds.; American Chemical Society: Washington, 1997, p. 423.
14. Richter, R. C.; Link, D.; Kingston, H. M. S.; *Anal. Chem.* **2001**, *73*, 30 A.
15. Zischka, M.; Kettisch, P.; Schalk, A.; Knapp, G.; *Fresenius' J. Anal. Chem.* **1998**, *361*, 90.
16. Bizzi, C. A.; Nobrega, J. A.; Barin, J. S.; Oliveira, J. S. S.; Schmidt, L.; Mello, P. A.; Flores, E. M. M.; *Anal. Chim. Acta* **2014**, *837*, 16.
17. Bizzi, C. A.; Nóbrega, J. A.; Barin, J. B. In *Microwave-Assisted Sample Preparation for Trace Element Determination*; Flores, E. M. M., ed.; Elsevier: Amsterdam, 2014, p. 179.
18. Robinson, J.; Kingman, S.; Irvine, D.; Licence, P.; Smith, A.; Dimitrakis, G.; Obermayer, D.; Kappe, C. O.; *Phys. Chem. Chem. Phys.* **2010**, *12*, 4750.
19. Krushevska, A.; Barnes, R. M.; Amarasiriwaradena, C. J.; Foner, H.; Martines, L.; *J. Anal. At. Spectrom.* **1992**, *7*, 845.
20. Gouveia, S. T.; Silva, F. V.; Costa, L. c. M.; Nogueira, A. R. A.; Nóbrega, J. A.; *Anal. Chim. Acta* **2001**, *445*, 269.
21. Bizzi, C. A.; Barin, J. S.; Garcia, E. E.; Nóbrega, J. A.; Dressler, V. L.; Flores, E. M. M.; *Spectrochim. Acta, Part B* **2011**, *66*, 394.
22. *Multiwave 3000: Microwave Sample Preparation Cook Book;* Anton Paar GmbH, Graz, 2003, p. 322.
23. McQuarrie, D. A.; Simon, J. D.; *Physical Chemistry: A Molecular Approach*; University Science Books: Sausalito, CA, 1997, p. 965.
24. Atkins, P.; de Paula, J.; *Elements of Physical Chemistry*; W. H. Freeman and Co.: New York, 2009, p. 578.
25. Shreve, R. N.; Austin, G. T.; *Shreve's Chemical Process Industries*; McGraw-Hill: New York, 1987, p. 717.
26. Smith, T. N.; Hash, K.; Davey, C.-L.; Mills, H.; Williams, H.; Kiely, D. E.; *Carbohydr. Res.* **2012**, *350*, 6.

Submitted: October 10, 2016
Published online: January 24, 2017

FAPERGS/CAPES has sponsored the publication of this article.